

## Band structure and semiconducting properties of FeSi

L. F. Mattheiss and D. R. Hamann

*AT&T Bell Laboratories, Murray Hill, New Jersey 07974*

(Received 21 December 1992)

The results of linear augmented-plane-wave band calculations for cubic FeSi, carried out in the local-density approximation, predict a small ( $\sim 0.11$  eV) indirect semiconductor gap which agrees well with empirical estimates ( $\sim 0.13$  eV). The origin of this gap, which occurs within the Fe ( $3d$ ) manifold, can be traced to a pseudogap that is present in the reference rocksalt phase that underlies the lower-symmetry FeSi structure. The relationship between the FeSi band structure and several types of many-body correlation mechanisms that have been advanced to explain its anomalous temperature-dependent magnetic properties is discussed.

### I. INTRODUCTION

Interest in FeSi dates back to the late 1930s when Föex<sup>1</sup> discovered that the magnetic susceptibility of this compound increased with temperature above room temperature. These observations were later confirmed by Benoit,<sup>2</sup> who proposed that the broad susceptibility maximum that was observed near 170 °C was due to an anti-ferromagnetic transition. However, the results of subsequent neutron-diffraction measurements<sup>3</sup> at both room and liquid-nitrogen temperatures failed to confirm the presence of long-range antiferromagnetic order in this system. Subsequent studies of the Mössbauer effect and Knight shift confirmed the absence of any sort of ordered moment.<sup>4</sup>

Theoretical expressions based on two (extremely similar) models were shown<sup>5</sup> to provide good fits to the temperature dependencies of the susceptibility and a related specific-heat anomaly in FeSi. The model contains two bands of noninteracting electrons, symmetrically placed about the Fermi level and split by a gap of  $\sim 0.13$  eV. Each band is capable of holding two electrons and has a bandwidth  $w$  that is *negligibly small compared to the gap*. (The authors considered this bandwidth requirement to be physically unreasonable,<sup>5</sup> and preferred to regard the model as one of thermally excited localized spins.) Subsequently, the inclusion of strong local Coulomb interactions was shown<sup>6</sup> to promote enhanced thermally induced spin fluctuations, which could explain the data qualitatively within a two-band model with narrow but not unreasonable bandwidths ( $\sim 1$  eV). However, the small gap was still required as a characteristic of the noninteracting density of states.<sup>6</sup>

Inelastic-neutron-scattering experiments<sup>7</sup> have now confirmed the picture of thermally induced spin fluctuations in FeSi. In a recent study of spin fluctuations in the rare-earth compound CeNiSn, which is considered to be a so-called "Kondo insulator," characteristics analogous to the FeSi fluctuation spectrum were noted.<sup>8</sup> On this basis, these authors<sup>8</sup> have suggested that FeSi might represent the first example of a transition-metal (as opposed to a rare-earth) Kondo insulator.<sup>9</sup> Such systems are considered to be related to heavy-fermion metals, and the

prospect of studying the complex many-body phenomena associated with this class of materials within the family of transition-metal compounds at room temperature and above is an exciting possibility.

An overview of the electronic properties for the Fe-Si system, one that spans the complete range of composition from the Fe to the Si-rich phases, suggests that the local-density-approximation (LDA) band theory provides a good description of many properties. For example, it has been shown<sup>10</sup> that local-spin-density band calculations provide a detailed understanding of the itinerant ferromagnetism that occurs in the Fe-rich face-centered-cubic (fcc) compound Fe<sub>3</sub>Si. Furthermore, band calculations<sup>11</sup> for the Si-rich semiconducting compound  $\beta$ -FeSi<sub>2</sub> have been equally successful. Despite a complicated orthorhombic structure that contains a total of 16 formula units per primitive cell, these calculations yield theoretical values for the FeSi<sub>2</sub> semiconductor gap [ $\sim 0.44$  and 0.80 eV in Refs. 11(a) and 11(b), respectively] that are in good-to-excellent agreement with the optical value ( $\sim 0.85$  eV). Finally, a self-consistent augmented-plane-wave (APW) band calculation<sup>12</sup> for the isostructural compound MnSi yields a small ( $\sim 0.12$  eV) energy gap at a band filling that is appropriate for FeSi.

The purpose of the present investigation is to determine the LDA band structure and properties of FeSi using a first-principles approach in order to provide a more rigorous starting point for understanding the magnetic behavior of this material. With this objective, a scalar-relativistic version<sup>13</sup> of the linear augmented-plane-wave (LAPW) method<sup>14</sup> has been applied to calculate the energy bands for the observed cubic as well as a simplified rocksalt version of the FeSi structure. In these calculations, exchange and correlation effects have been included with the use of Wigner interpolation formula.<sup>15</sup>

### II. CALCULATIONAL DETAILS

The FeSi structure is moderately complicated and particularly difficult to visualize. Its characteristic features are illustrated in Fig. 1. The primitive cell contains four FeSi formula units. The local coordination at the individual Fe and Si sites is best described in terms of a

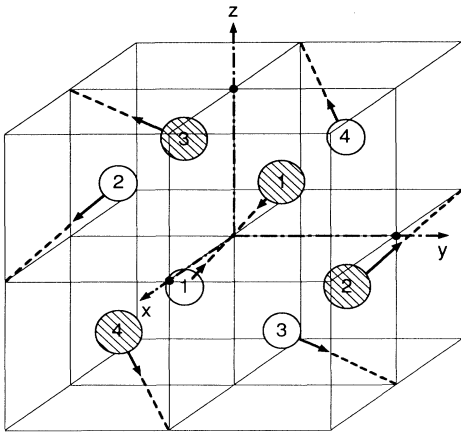


FIG. 1. Simplified representation of the simple-cubic primitive unit cell for the FeSi structure [space group  $P2_13(T^4)$ ] in which the actual Fe (shaded circles) and Si (open circles) atom positions are represented as [111]-type displacements from those of a reference rock-salt structure. The resulting nearest-neighbor bonds involve like-numbered Fe( $n$ )-Si( $n$ ) pairs that are located either within the central cell ( $n=1$ ) or across the cell-boundary edges ( $n=2-4$ ).

pairing-type distortion of an underlying rock-salt structure in which the individual constituents are displaced along [111] directions so as to change the rock-salt third neighbors (i.e., those along the cube diagonals) into FeSi nearest neighbors. These displacements reduce the space-group symmetry<sup>3</sup> from  $Fm\bar{3}m(O_h^5)$  to  $P2_13(T^4)$  in such a way that the Bravais lattice is simple cubic but the overall point symmetry is tetrahedral.

Both the Fe and Si atoms are situated at the  $4(a)$ -type sites in the simple-cubic unit cell, with position coordinates  $(u, u, u)$ ,  $(\frac{1}{2}+u, \frac{1}{2}-u, \bar{u})$ ,  $(\bar{u}, \frac{1}{2}+u, \frac{1}{2}-u)$ , and  $(\frac{1}{2}-u, \bar{u}, \frac{1}{2}+u)$ . The FeSi lattice parameter ( $a=4.493$  Å) has been determined from neutron-diffraction measurements<sup>3</sup> at liquid-nitrogen temperature. The corresponding values for the internal atom-position parameters,  $u(\text{Fe})=0.1358$  and  $u(\text{Si})=0.844$ , were evaluated<sup>3</sup> from data taken at higher temperatures ( $\sim 300^\circ\text{C}$ ). Similar values for these structural parameters [i.e.,  $a=4.489$  Å,  $u(\text{Fe})=0.137$ , and  $u(\text{Si})=0.842$ ] were determined in an earlier single-crystal x-ray-diffraction study.<sup>16</sup>

It should be emphasized that the displacements involved in forming the FeSi structure from the reference rock-salt structure are sizeable. For comparison, the rock-salt atom-position parameters correspond to the values  $u(\text{Fe})=0.25$  and  $u(\text{Si})=0.75$ , respectively. In this high-symmetry rock-salt phase, each Fe has six Si neighbors at  $\sim 2.25$  Å, 12 Fe's at  $\sim 3.18$  Å, and eight Si's at  $\sim 3.89$  Å. After the FeSi-type displacements, Fe has seven Si neighbors (including one at  $\sim 2.27$  Å, three at  $\sim 2.35$  Å, and three at  $\sim 2.52$  Å), as well as six (out of the original 12) more-distant Fe neighbors at  $\sim 2.75$  Å.

The point symmetry at the Fe and Si sites is  $C_3$ , which is a cyclic group of order three that consists of  $120^\circ$  rotations about an appropriate [111] axis and its powers. The  $P2_13$  space group is nonsymmorphic and contains 12

symmetry operations. The space-group operations that involve  $C_3$  are associated with primitive translations. However, the remaining operations in the tetrahedral point group  $T$  are combined with one of the three nonprimitive translations,  $\tau=(\frac{1}{2}, \frac{1}{2}, 0)$ ,  $(\frac{1}{2}, 0, \frac{1}{2})$ , and  $(0, \frac{1}{2}, \frac{1}{2})$ . These serve to restore the lattice when the [111]-oriented Fe(1)-Si(1) bond in Fig. 1 is rotated to an alternate [111] axis, one that matches an equivalent nearest-neighbor Fe( $n$ )-Si( $n$ ) bond direction ( $n=2-4$ ).

In the present study, LAPW calculations have been carried out both for the undistorted rock-salt structure as well as the actual FeSi structure that is shown in Fig. 1. To simplify the discussion, the rock-salt-type FeSi results will be designated FeSi(fcc), since the rock-salt Bravais lattice is fcc. The corresponding results for the proper FeSi structure will be identified as FeSi(sc), where sc refers to the simple-cubic Bravais lattice in Fig. 1. Results for a nonprimitive rock-salt structure that contains four FeSi formula units will be designated  $\text{Fe}_4\text{Si}_4(\text{fcc})$ .

In the present implementation of the LAPW method, there are no shape approximations imposed on either the crystalline charge density or the potential.<sup>13</sup> The cutoffs have been set at values such that the FeSi(sc) calculations include a basis of  $\sim 430$  LAPW's (12-Ry plane-wave cutoff) and spherical-harmonic terms through  $l=6$ . The crystalline charge density and potential have been expanded with about 4200 plane waves (55-Ry cutoff) in the interstitial region and lattice harmonics with  $l_{\text{max}}=4$  within the muffin-tin spheres. A five-point  $k$  mesh in the irreducible  $1/24$  wedge (reduced by time-reversal symmetry<sup>17</sup>) has been used to carry out Brillouin-zone integrations. Analogous LAPW parameters have been used in the corresponding rock-salt-structure calculations. In both cases, the Fe  $3d^7 4s^1$  and Si  $3s^2 3p^2$  states are treated as valence electrons whereas the more tightly bound levels are included via a frozen-core approximations.<sup>13</sup>

### III. RESULTS

The LAPW band results for FeSi(sc) are plotted along symmetry lines in the simple-cubic (sc) Brillouin zone in Fig. 2. Those bands with predominant Fe  $3d$  and Si  $3s, 3p$  orbital character are identified by square and triangle symbols, respectively. The lowest grouping of four bands evolves essentially from the Si ( $3s$ ) states. The bands above these at slightly higher ( $\sim -6$  to  $-3$  eV) energies reflect Si-Fe hybridization effects and their mixed character is denoted by the solid dots. The Fe  $3d$  bands span the adjoining energy range from about  $-3$  to  $+3$  eV, while hybridized bands with enhanced Si  $3p$  character reappear at higher energies near the top of Fig. 2.

As expected, the FeSi Fermi level occurs in the midst of the Fe  $3d$  bands. In fact, the 48 valence electrons per cell are just sufficient to fill completely the lowest 24 valence bands. These are most easily "counted" along the  $Z$ ,  $RM$ , and  $Z'$  lines, where each of the bands is two-fold degenerate as a result of the nonsymmorphic character of the  $P2_13$  space group.<sup>18</sup> As is well known, such degeneracies can occur in the case of nonsymmorphic space groups for states with wave vectors on the Brillouin-zone faces where bands can "stick" together.

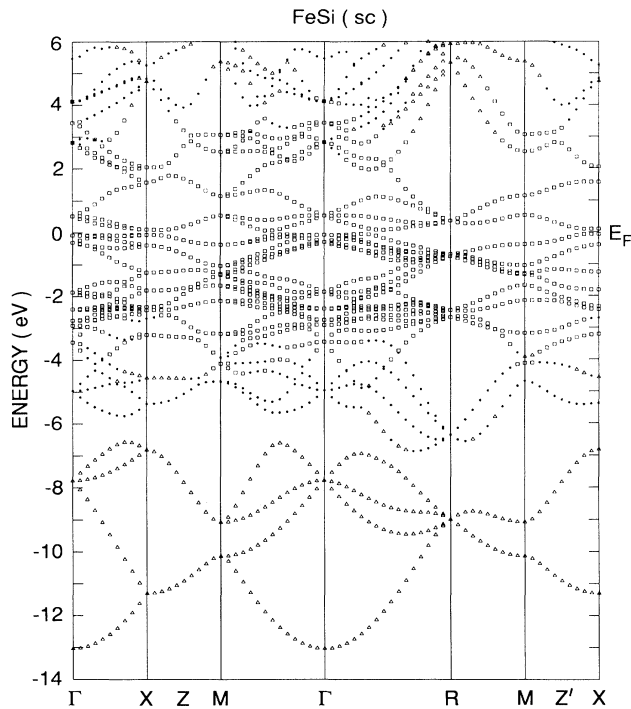


FIG. 2. LAPW energy-band results for FeSi(sc) with the observed tetrahedral structure that contains four FeSi formula units per simple-cubic cell. In units of  $(\pi/a)$ , the inequivalent Z and Z' lines (which are distinct because of the tetrahedral point symmetry) correspond to the  $(1, \alpha, 0)$  and  $(1, 0, \alpha)$  directions, respectively. Bands with significant Fe 3d or Si 3s, 3p orbital character are labeled with squares ( $w_d > 30\%$ ) and triangles ( $w_{s,p} > 15\%$ ), respectively.

The present LAPW bands for FeSi(sc) are in excellent agreement with the APW results that have been calculated previously<sup>12</sup> for the isostructural compound MnSi. According to these earlier results, a comparable indirect gap of  $\sim 0.12$  eV occurs between the 24th and 25th bands in MnSi. However, this gap occurs above the MnSi Fermi level since this system contains four fewer valence electrons per unit cell.

A more detailed view of the FeSi(sc) bands near  $E_F$  is provided in Fig. 3 where the results are replotted with an expanded energy scale. The calculated minimum gap is indirect and has a magnitude of about 0.11 eV. It involves the valence-band maximum along the  $\Gamma R$  line and the conduction-band minimum along  $\Gamma M$ . The minimum direct gap ( $\sim 0.14$  eV) occurs along  $\Gamma M$ . The calculated indirect-gap value is close to the empirical value of  $\sim 0.13$  eV that is generally attributed<sup>5</sup> to FeSi. As discussed below, the results of supplementary studies show that the theoretical value for the FeSi gap is sensitive to the specific values of the atom-position parameters  $u(\text{Fe})$  and  $u(\text{Si})$ . Thus, a comprehensive LDA structural determination will be required before a precise theoretical value for the FeSi LDA band gap can be evaluated.

An unusual feature of the bands near the FeSi Fermi level involves the fact that several valence-band (conduction-band) maxima (minima) occur within a few meV of the gap edge. This suggests that the density of

states (DOS) near the gap will be extremely sharp, increasing rapidly to rather large values over relatively small energy increments. Furthermore, exploratory calculations have shown that relatively small changes ( $\sim 0.005$ ) in the  $u(\text{Fe})$  and  $u(\text{Si})$  atom-position-parameter values cause the energies of these nearly degenerate band-edge states to shift relative to one another by tens of meV. These changes may be sufficient to alter the magnitude and perhaps the location of the calculated indirect gap. More importantly, they may also modify the detailed shape of the FeSi DOS curve near  $E_F$ .

An overview of the calculated DOS characteristics for the present LAPW FeSi(sc) bands of Figs. 2 and 3 is shown in Fig. 4. It is evident that the Si-projected component (lowest panel) scales with the total DOS (top panel) in the low- and high-energy ranges whereas the Fe 3d component becomes dominant near  $E_F$ . The  $E(\mathbf{k})$  mesh that has been applied in the present DOS calculation is too coarse to provide a quantitative representation of DOS features near  $E_F$  since it involves  $\Delta k$  increments that are one-third the  $\Gamma X$  dimension in Figs. 2 and 3. It is clear from the band details in Fig. 3 that a much finer  $\mathbf{k}$  sampling would be required in order to obtain a quantitative determination of the energy-dependent DOS near  $E_F$  for FeSi(sc).

In order to provide a better understanding of the origin and nature of the calculated semiconductor gap in FeSi(sc), it is useful to consider the band properties of the undistorted phase with the symmetry of the rocksalt structure. The LAPW band results for FeSi(fcc) are plotted along symmetry lines in the fcc Brillouin zone in Fig. 5. There is now only one formula unit per cell and the nine bands in this 20-eV energy range originate from the Fe 3d and Si 3s, 3p states. Of particular importance are the doubly degenerate  $X_5$  and  $X_5'$  bands that bracket  $E_F$ . These have predominant Fe 3d and Si 3p character, respectively.

The importance of this  $X_5$ - $X_5'$  band alignment arises from the fact that the transformation from the rocksalt to the FeSi(sc) structure involves two steps. The first is a

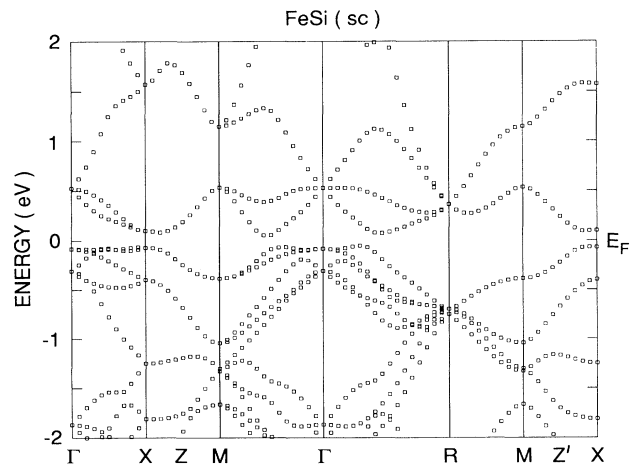


FIG. 3. Expanded plot of the FeSi(sc) bands near  $E_F$ , with orbital character labeled in accordance with Fig. 2.

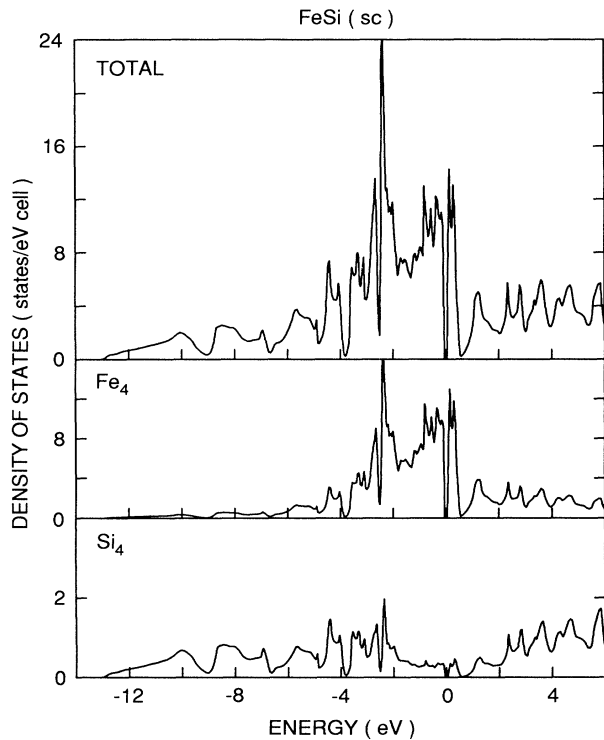


FIG. 4. Total and muffin-tin-projected density-of-states results for FeSi(sc) which have been calculated with the use of tetrahedral interpolation based on LAPW results at 216 points in the full Brillouin zone.

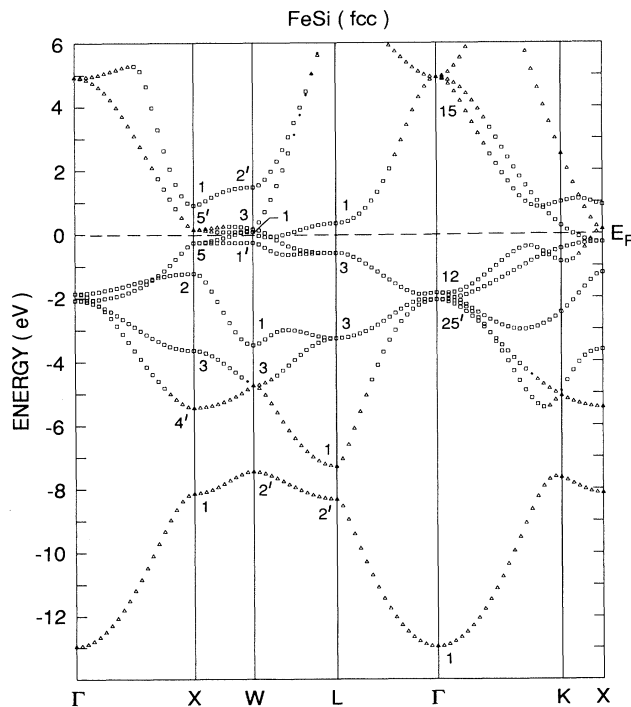


FIG. 5. LAPW energy-band results for FeSi(fcc) with an undistorted rocksalt structure that contains one formula unit per primitive fcc cell. Band labeling is in accordance with Fig. 2.

fourfold increase in the size of the primitive unit cell. In band-structure terms, this involves the folding of the fcc zone-boundary  $X$  points into the zone-center  $\Gamma$ . As a result, the twofold degeneracies near the FeSi(fcc) Fermi level are increased to sixfold degeneracies in the FeSi(sc) phase. The subsequent Fe and Si atom displacements from their rocksalt positions reduce the space-group symmetry and thereby introduce additional interactions between states that were noninteracting originally because of symmetry.

The extent to which this simple picture replicates the actual band properties of FeSi(sc) is illustrated in Fig. 6, where the appropriately folded rocksalt bands of Fig. 5 are replotted along symmetry lines of the sc Brillouin zone. A comparison with the LAPW FeSi(sc) bands in Fig. 2 reveals many qualitative similarities. The reduced symmetry that is caused by the changes in  $u(\text{Fe})$  and  $u(\text{Si})$  from their rocksalt values produces band shifts in Fig. 2, but the overall distribution of bands in the two figures remains visually similar.

The results in Fig. 6 show that the rocksalt variant of FeSi is a semimetal, containing small compensating electron and hole pockets near  $\Gamma$  and  $X$  in the folded sc zone. As shown by the corresponding DOS results in Fig. 7, the FeSi(fcc) Fermi level lies in a pseudogap that occurs near the top of the Fe 3d manifold. These results demonstrate that the FeSi(fcc)-FeSi(sc) distortion is not driven by Fermi-surface effects that are predominant, for example, in systems that undergo charge-density-wave distortions or Peierls transitions. Experimentally, this is supported by the fact that this same FeSi structure occurs<sup>19</sup> for the entire series of compounds CrSi, MnSi, FeSi, and CoSi,

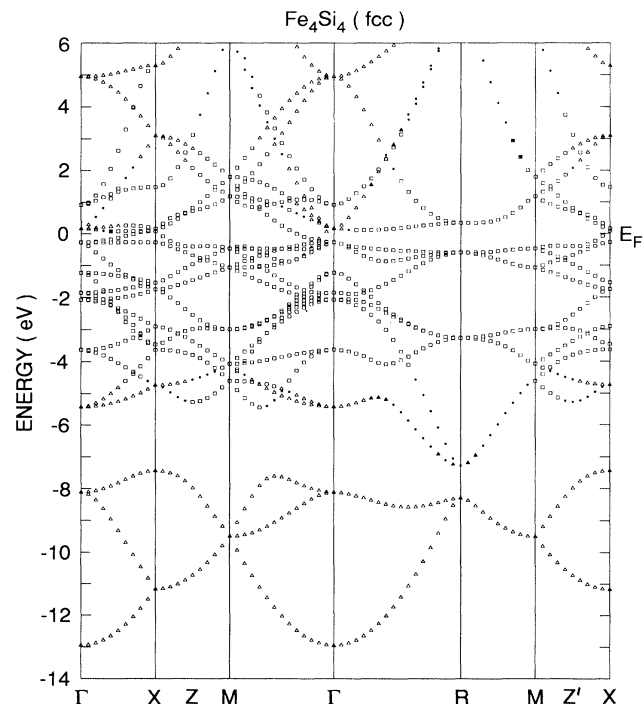


FIG. 6. Folded rocksalt-structure bands for Fe<sub>4</sub>Si<sub>4</sub>(fcc) in a nonprimitive simple-cubic cell that contains four FeSi formula units. Band labeling is in accordance with Fig. 2.

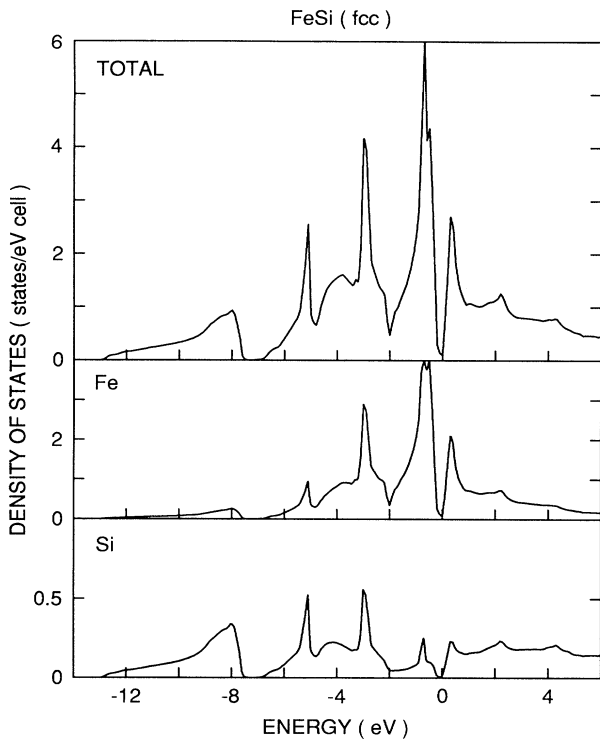


FIG. 7. Total and muffin-tin-projected density-of-states results for the undistorted rocksalt variant of FeSi(fcc) which have been calculated with the use of tetrahedral interpolation based on LAPW results at 44  $\mathbf{k}$  points in the  $1/48$  irreducible wedge of the fcc Brillouin zone.

where the average number of filled bands increases from 20 to 26. The calculated LDA energy difference between the model rocksalt and distorted sc phase of FeSi is large,  $\sim 1.6$  eV/formula unit. Thus, there is no reason to expect that FeSi will revert to the more symmetric rocksalt structure at high temperatures.

#### IV. DISCUSSION

The LDA results that are presented here form a basis for considering the respective roles played by the “mean-field” (LDA) and many-body correlation effects in determining the magnetic properties of FeSi. It is clear from the outset that these LDA results do not by themselves yield the model DOS which Jaccarino *et al.*<sup>5</sup> postulated to fit the temperature dependence of the susceptibility. The LDA gap is comparable to the gap of their model, but the model requires extremely narrow valence and conduction bands that each hold two electrons per Fe and whose widths are small compared to the gap. As is readily seen from Figs. 3 and 4, the relatively sharp peaks that exist in the LDA DOS have widths of  $\sim 0.5$  eV, about five times the gap, and each can accommodate approximately one electron per Fe. We conclude that the ordinary band results cannot explain even qualitatively the anomalous temperature dependence of the FeSi susceptibility.

The present band DOS results provide a reasonable starting point for the many-body treatment of Takahashi

and Moriya.<sup>6</sup> In their model, a mean-field gap comparable to the empirical gap is still required to set the energy scale for the temperature dependence. However, bandwidths of  $\sim 1$  eV are assumed, and the susceptibility, which would be thermally activated but small in the noninteracting system, is strongly enhanced ferromagnetically by the local Coulomb interaction. This yields the desired susceptibility, and, qualitatively at least, the thermally activated spin fluctuations observed by neutron diffraction.<sup>7</sup> Takahashi and Moriya<sup>6</sup> made no attempt to extract detailed parameters to fit experiment within their treatment. From a comparison of the DOS features near  $E_F$  for the fcc and sc forms of FeSi in Figs. 4 and 7, it is clear that the near-gap structure is sharpened in the distorted sc phase. Temperature dependence of this structure due to thermal variations in  $u(\text{Fe})$  and  $u(\text{Si})$  would be amplified by the Coulomb interaction, and could also play a role in enhancing the temperature dependence of observed properties.

It has been suggested<sup>8</sup> that an alternative many-body model, that of the Kondo insulator, may apply to FeSi. This observation is based on similarities of its spin-fluctuation spectrum to that of CeNiSn, one of the several rare-earth compounds that is considered to be in this category.<sup>8</sup> In this class of models, a set of localized atom-like electron levels is coupled to a separate broadband of itinerant states. In FeSi, these roles would be played by the Fe 3*d* states and Si 3*s*-3*p* bands, respectively. The localized states are assumed to have strong intra-atomic Coulomb interactions. For a general electron filling, such systems form local spins which tend to be screened by the band electrons, as in the isolated-impurity Kondo effect. These localized spins are antiferromagnetically coupled to each other through the band electrons. This combination of competing effects leads to a rich variety of behaviors, including the coherent heavy-fermion state at low temperatures.<sup>8</sup> However, for the filling that would make this two-band model a semiconductor in the absence of the Coulomb interaction, the gap is preserved<sup>9</sup> and the magnetic interactions appear to vanish at low temperatures.<sup>8</sup>

This class of models is extremely challenging, and no comprehensive theory exists. However, a series of exact-diagonalization studies on (very) small versions of such models by Jullien and Martin<sup>9</sup> have shown that the exact ground state is the analytic continuation of the noninteracting state, so presumably the noninteracting (more properly, mean field) bands should be the relevant starting point for a theoretical treatment of FeSi in this context. The Jullien-Martin analysis shows that there is an extreme renormalization of the bandwidths, so that the present LDA bands could be narrowed considerably, perhaps to the extent required to emulate the Jaccarino *et al.*<sup>5</sup> model DOS. However, the gap is only modestly renormalized, which is consistent with our result that the LDA gap is comparable to the empirical value. The Kondo-insulator model seems qualitatively different from the enhanced spin-fluctuation model, and it is curious that the band results appear to be consistent with both. Sorting out these aspects of the problem is far beyond the scope of this paper.

If we neglect, for the moment, considerations of potentially strong magnetic correlation effects in FeSi and regard this compound as a conventional semiconductor, we must note that the LDA usually underestimates band gaps, often by a factor of 2. The fact that the LDA band gap for FeSi is in good agreement with empirical estimates suggests that this so-called “band-gap” problem<sup>20</sup> is not a severe one in this compound. A similar situation occurs in another small-gap transition-metal silicide semiconductor CrSi<sub>2</sub>, where the calculated<sup>21</sup> indirect gap of 0.30 eV is found to be in excellent agreement with the optical ( $\sim 0.35$  eV) value. It has been proposed<sup>21</sup> that the similar  $3d$  orbital characteristics of states on both sides of the band gap in compounds such as CrSi<sub>2</sub> and FeSi [and, perhaps,  $\beta$ -FeSi<sub>2</sub> (Ref. 11)] may make the nonlocal many-body corrections<sup>22</sup> to the LDA similar for both sets of states in these systems. How or whether this real materials way of looking at band-gap renormalization relates to that considered in the context of the highly idealized Kondo lattice model<sup>9</sup> is another topic beyond our scope.

To summarize, we have investigated the electronic properties of FeSi in the LDA by means of LAPW band calculations. The results predict that FeSi is a small-gap semiconductor with sharp DOS features near  $E_F$ . While the calculated LDA gap of  $\sim 0.11$  eV is close to the quoted experimental value of  $\sim 0.13$  eV, a definitive LDA determination must await a comprehensive evaluation of the FeSi low-temperature structural parameters. The unusual temperature dependence of the magnetic susceptibility of this compound is not accounted for by the LDA DOS results, suggesting that a fully satisfactory explanation may involve one of several models that have been proposed for incorporating strong correlation effects in novel magnetic systems such as FeSi.

#### ACKNOWLEDGMENTS

We are pleased to acknowledge that this investigation was stimulated by several valuable discussions with G. Aeppli.

- 
- <sup>1</sup>G. Föex, *J. Phys. Radium* **9**, 37 (1938).  
<sup>2</sup>R. Benoit, *J. Chim. Phys.* **52**, 119 (1955).  
<sup>3</sup>H. Watanabe, H. Yamamoto, and K. Ito, *J. Phys. Soc. Jpn.* **18**, 995 (1963).  
<sup>4</sup>G. K. Wertheim, V. Jaccarino, J. H. Wernick, J. A. Seitchik, H. J. Williams, and R. C. Sherwood, *Phys. Lett.* **18**, 89 (1965).  
<sup>5</sup>V. Jaccarino, G. K. Wertheim, J. H. Wernick, L. R. Walker, and S. Arajs, *Phys. Rev.* **160**, 476 (1967).  
<sup>6</sup>Y. Takahashi and T. Moriya, *J. Phys. Soc. Jpn.* **46**, 1451 (1979); S. N. Evangelou and D. M. Edwards, *J. Phys. C* **16**, 2121 (1983).  
<sup>7</sup>G. Shirane, J. E. Fisher, Y. Endoh, and K. Tajima, *Phys. Rev. Lett.* **59**, 351 (1987); K. Tajima, Y. Endoh, J. E. Fisher, and G. Shirane, *Phys. Rev. B* **38**, 6954 (1988).  
<sup>8</sup>T. E. Mason, G. Aeppli, A. P. Ramirez, K. N. Clausen, C. Broholm, N. Stücheli, E. Bucher, and T. T. M. Palstra, *Phys. Rev. Lett.* **69**, 490 (1992).  
<sup>9</sup>R. Jullien and R. M. Martin, *Phys. Rev. B* **26**, 6173 (1982).  
<sup>10</sup>A. C. Switendick, *Solid State Commun.* **19**, 511 (1976); A. R. Williams, V. L. Moruzzi, and C. D. Gelatt, Jr., *J. Appl. Phys.* **53**, 2019 (1982); J. Kudrnovsky, N. E. Christensen, and O. K. Andersen, *Phys. Rev. B* **43**, 5924 (1991).  
<sup>11</sup>(a) R. Eppenga, *J. Appl. Phys.* **68**, 3027 (1990); (b) N. E. Christensen, *Phys. Rev. B* **42**, 7148 (1990).  
<sup>12</sup>O. Nakanishi, A. Yanase, and A. Hasegawa, *J. Magn. Magn. Mater.* **15-18**, 879 (1980).  
<sup>13</sup>L. F. Mattheiss and D. R. Hamann, *Phys. Rev. B* **33**, 823 (1986).  
<sup>14</sup>O. K. Andersen, *Phys. Rev. B* **12**, 3060 (1975).  
<sup>15</sup>E. Wigner, *Phys. Rev.* **46**, 1002 (1934).  
<sup>16</sup>L. Pauling and A. M. Soldate, *Acta Crystallogr.* **1**, 212 (1948).  
<sup>17</sup>M. Lax, *Symmetry Principles in Solid State and Molecular Physics* (Wiley, New York, 1974).  
<sup>18</sup>A. P. Cracknell, B. L. Davies, S. C. Miller, and W. F. Love, *Kronecker Product Tables* (Plenum, New York, 1979), Vol. I.  
<sup>19</sup>D. Shinoda and S. Asanabe, *J. Phys. Soc. Jpn.* **21**, 555 (1966).  
<sup>20</sup>L. J. Sham and M. Schlüter, *Phys. Rev. Lett.* **51**, 1888 (1983); *Phys. Rev. B* **32**, 3883 (1985).  
<sup>21</sup>L. F. Mattheiss, *Phys. Rev. B* **43**, 1863 (1991).  
<sup>22</sup>R. W. Godby, M. Schlüter, and L. J. Sham, *Phys. Rev. Lett.* **56**, 2415 (1986); *Phys. Rev. B* **36**, 6497 (1987).